Tree Physiology 39, 1685–1695
doi:10.1093/treephys/tpz072

Research paper

Short-time xylem tension relaxation prevents vessel refilling and alleviates cryo-fixation artifacts in diffuse-porous *Carpinus tschonoskii* and *Cercidiphyllum japonicum*

Mayumi Y. Ogasa[1,2,5,7], Kenichi Yazaki[1], Yasuhiro Utsumi[3], Naoko H. Miki[4] and Kenji Fukuda[2,6]

[1]Department of Plant Ecology, Forestry and Forest Products Research Institute, Tsukuba 305-8687, Japan; [2]Department of Natural Environmental Studies, Graduate School of Frontier Sciences, The University of Tokyo, Kashiwa 277-8563, Japan; [3]Kyushu University Forest, Kyushu University, Ashoro 089-3705, Japan; [4]Department of Environmental Ecology, Graduate School of Environmental and Life Science, Okayama University, 1-1-1 Tsushimanaka, Kita-ku, Okayama 700-8530, Japan; [5]Present address: Forest Ecology Group, Kansai Research Center, Forestry and Forest Products Research Institute, 68 Nagaikyutaroh, Momoyama, Fushimi-ku, Kyoto, Kyoto 612-0855, Japan; [6]Present address: Department of Forest Science, Graduate School of Agricultural and Life Sciences, The University of Tokyo, 1-1-1 Yayoi, Bunkyo-ku, Tokyo 113-8657, Japan; [7]Corresponding author (mayumiogasa@ffpri.affrc.go.jp) http://orcid.org/0000-0002-3814-4937 http://orcid.org/0000-0002-9980-3107

Received December 18, 2018; accepted June 12, 2019; handling Editor Kathy Steppe

Xylem tension relaxation is an important procedure that closely resembles the in vivo xylem water distribution when measuring conductivity or observing water distribution of plant tissue samples by cryo-scanning electron microscopy (cryo-SEM). Recent studies have shown that partial xylem embolism occurs when samples under tension are cut under water and that gas-filled vessels are refilled during tension relaxation. Furthermore, the frequency of gas-filled vessels has been reported to increase in samples without tension relaxation before cryo-fixation by liquid nitrogen, particularly in samples with significant tension. Here, we examined the effect of tension relaxation on these artifacts in *Carpinus tschonoskii* and *Cercidiphyllum japonicum* using magnetic resonance imaging. We observed that xylem embolism rarely occurs in bench-dried samples cut under water. In both species, a small portion of the xylem was refilled within ~1 h after tension relaxation. Cryo-SEM observations revealed that short-time (<1 h) xylem tension relaxation decreases the frequency of gas-filled vessels in samples frozen after xylem tension relaxation regardless of the water potential compared with that in samples frozen without rehydration in both species. Therefore, short-time tension relaxation is necessary to retain xylem water distribution during sample preparation against artifacts.

Keywords: cryo-SEM, freezing, MRI, tension-cutting artifact, xylem water distribution.

Introduction

Long-distance water transport in woody species is controlled by pressures well below vapor pressure (Dixon and Joly 1895), causing transport systems to be vulnerable to xylem cavitation (Tyree and Sperry 1989, Tyree and Zimmermann 2002). According to previously reported measurements of plant water potential using a Scholander–Hammel pressure bomb (Scholander et al. 1965, Turner 1988), water within the conduits of a branch/stem that is cut in air is withdrawn up to the conduit end under atmospheric pressure (Tyree and Zimmermann 2002, Venturas et al. 2017). Therefore, when evaluating the water transport function by hydraulic conductivity measurements of excised branch segments or dye perfusion, the procedure used to cut or notch under water (dye solution) is required to retain in vivo xylem water distribution (Sperry et al. 1988, Sano et al. 2005).

Xylem aspiration of air has been reported to occur in open vessels at the cut end of the branch when cutting under water

with branch samples remaining under tension. This effect is termed 'tension-cutting artifact' (Wheeler et al. 2013, Rockwell et al. 2014, Venturas et al. 2014) and was recently confirmed using imaging techniques, including magnetic resonance imaging (MRI) and X-ray microtomography (Cochard et al. 2014, Torres-Ruiz et al. 2015, Ogasa et al. 2016). Xylem tension relaxation before excising a measured segment is recommended to alleviate tension-cutting artifacts (Dixon and Joly 1895, Cochard and Tyree 1990, Wheeler et al. 2013, Melcher 2015). These artifacts can be avoided by cutting stems under water at a position farther from the position of interest, i.e., at a length greater than the maximum vessel length (MVL) of the species. The effect of artifacts on xylem conductivity appears to depend on the species, organ and the intensity of tension (Trifilò et al. 2014, Venturas et al. 2014, Scoffoni and Sack 2015, Savi et al. 2017).

Tension relaxation of a sample with the cut end simultaneously immersed in water may result in refilling of gas-filled vessels (Trifilò et al. 2014, Venturas et al. 2014). In fact, vessel refilling after stem cutting of *Vitis coingetiae* under water has been confirmed by MRI (Ogasa et al. 2016). This can result in xylem transport function overestimation. Eliminating tension-cutting artifacts and 'refilling artifacts' during sample preparation is necessary to accurately measure xylem hydraulic function.

Furthermore, xylem tension relaxation is recommended during sample preparation to observe xylem water distribution by cryo-scanning electron microscopy (cryo-SEM) (Cochard et al. 2000). Cryo-SEM is an effective tool for observing water distribution in conduit lumina at a viewing surface because it enables investigators to count gas-filled (or water-filled) conduits at the cellular level and detecting the distribution of embolized (or water-filled) xylem areas at the tissue level (Utsumi et al. 1998, 1999, 2003, Mayr and Cochard 2003, Cobb et al. 2007, Nagai and Utsumi 2012). To stabilize the presence or absence of water in the lumen and maintain the cell structure, samples are immersed into liquid nitrogen (LN_2; Utsumi and Sano 2014). However, if the samples are frozen when they remain under tension during transpiration or dehydration, water-filled conduits may alter their states on the viewing surface for cryo-SEM to be empty or contain air bubbles or scattered water (ice) particles, which is impossible in vivo within their lumina (Cochard et al. 2000, Umebayashi et al. 2015). These 'cryo-fixation artifacts' have been reported to be decreased by xylem tension relaxation before freezing the sample by LN_2 plunging (Cochard et al. 2000, Umebayashi et al. 2015). However, previous studies have not considered the effects of the extent of tension-cutting and refilling artifacts on xylem water distribution of samples after cryo-fixation. In addition, whether obtaining various lumen states by cryo-fixation artifacts depends on the xylem tension before freezing remains unclear. The effect of the extent of tension relaxation on the decrease in each conduit content state has not been evaluated quantitatively at a cellular (vessel) level. Long periods of sample rehydration for xylem tension relaxation can result in conduit refilling. Tension-cutting artifacts must be eliminated during sample harvest. Thus, samples for cryo-fixation must be free of refilling, tension-cutting and cryo-fixation artifacts.

In this study, we first examined the effect of cutting under water on the extent of tension-cutting and refilling artifacts by monitoring xylem water distribution before and after stem cutting under water using noninvasive MRI of two diffuse-porous tree species, *Carpinus tschonoskii* and *Cercidiphyllum japonicum*. These two species were used because the presence/absence of water in the xylem is detectable by MRI according to our preliminary experiments on >10 diffuse-porous species. Further, we determined the effects of xylem tension relaxation on the occurrence and magnitude of cryo-fixation artifacts by comparing the ratio of gas-filled conduits between tension-relaxed and control samples.

Materials and methods

Plant materials

For Experiment 1, branch samples with leaves of *C. tschonoskii* and *C. japonicum* were collected from trees measuring at least 5 m in heights at the Kashiwa campus of The University of Tokyo, Kashiwa, Japan. The cut end of each branch sample was immediately sealed using Vaseline, and samples were wrapped in plastic bags and transported to the laboratory. The *C. tschonoskii* and *C. japonicum* samples were 1.1–1.8 m (n = 6) and 1.2–1.9 m (n = 6) in length, respectively. Potted seedlings of both species were used for Experiment 2. All seedlings were grown under sufficient irrigation in the experiment field at the Kashiwa campus of The University of Tokyo. The *C. tschonoskii* and *C. japonicum* seedlings were 1.0–1.4 m (n = 12) and 1.3–2.0 m (n = 10) in height, respectively. Branch samples with similar sizes were collected from plants grown in the arboretum of the Forestry and Forest Products Research Institute, Tsukuba, Japan, and used for Experiment 2. These branches were subjected to cryo-fixation at a low rate (n = 2 per species). All experiments were conducted in the summer of 2013–15.

Maximum vessel length measurement

Maximum vessel length (MVL) was measured using the air injection method (Zimmerman and Jeje 1981) with three and four stem samples of potted *C. tschonoskii* and *C. japonicum* seedlings, respectively. The long main axis was excised and flushed with 20-mM KCl solution at 100 kPa for 30 min to refill gas-filled vessels that may pass air. Further, air was applied at 80 kPa from the distal cut end. The basal end was immersed in water and cut back at 1-cm increments until air bubbles appeared. MVL was defined as the remaining axis length.

Magnetic resonance imaging

The MRI analysis was conducted on a sample axis wrapped with a solenoid coil using a compact MRI instrument with field strength of 1.0 T (MRTechnology Inc., Tsukuba, Japan). We used proton density-weighted spin-echo sequences with 2000-ms repetition time (TR) and 13-ms echo time (TE) to image *C. tschonoskii* and 1000-ms TR and 11-ms TE to image *C. japonicum*. Two-dimensional images of 256 × 256 pixels with a voxel size of 33 μm × 33 μm × 1 mm were obtained for *C. tschonoskii*, whereas images of 256 × 128 pixels with a voxel size of 67 μm × 67 μm × 1 mm were obtained for *C. japonicum*. Gradient amplitude and active shimming parameters were fixed during MR imaging of each sample. Each MR image of *C. tschonoskii* and *C. japonicum* required ∼55 min and 13 min, respectively.

Cryo-SEM observation

To recognize water-filled xylem cells, an MR image was compared with a cryo-SEM image for each species (Figure 1). Branch axes or potted seedling stems were frozen directly with LN_2 filled in plastic collars that were attached to the branch axis/stem. Frozen stem segments were sampled after 5 min of freezing and stored at −80 °C until the cryo-SEM observations were conducted. Disc specimens were cryoplaned using a cryostat-microtome (HM505E, Microm, Walldorf, Germany) attached to a sample holder with Tissue-Tek O.C.T. Compound (Sakura Finetek Japan, Tokyo, Japan) and set into the cryo-SEM system (JSM-6510 attached with a cryo-SEM unit, JEOL, Tokyo, Japan) according to the procedure reported by Utsumi and Sano (2014) and Yazaki et al. (2019). Surfaces of the specimens were freeze-etched at −95 °C for a few minutes on the cold stage in the cryo-SEM to clearly reveal cell outlines (Yazaki et al. 2017, 2019). Secondary electron images were observed without coating under an accelerating voltage of 3 kV on the cold stage at ca −130 °C.

Experiment 1: tension-cutting and refilling artifact observations by MRI

The design of Experiment 1 was based on Ogasa et al. (2016). In brief, a bench-dried branch axis with leaves installed in MRI was gently cut back several times under water at an upstream position <MVL from the MR imaging point, while a compact MRI unit was lowered using a hand lifter (see Figure S1A available as Supplementary Data at *Tree Physiology* Online). Water distribution patterns were compared between MR images obtained before and after branch cutting at the same position to confirm vessel content displaced by air from water as a tension-cutting artifact (n = 3 per species). To examine the reducing effects of tension-cutting artifacts, a similar experiment was conducted; however, the branch axis was cut at a position >MLV from the MR imaging point (n = 3 per species). Xylem water distribution in the branch samples were monitored by MRI every 1 h for *C. tschonoskii* or 30 min for *C. japonicum*, and the experiment was initiated after detecting xylem cavitation in each sample. Leaf water potential (Ψ_{leaf}) was measured immediately after obtaining MR images before and after cutting in a pressure chamber (Model 1000, PMS Instrument Co., Corvallis, OR, USA).

To assess vessel refilling during tension relaxation after cutting under water, MR images were acquired periodically after cutting and compared with those acquired immediately after

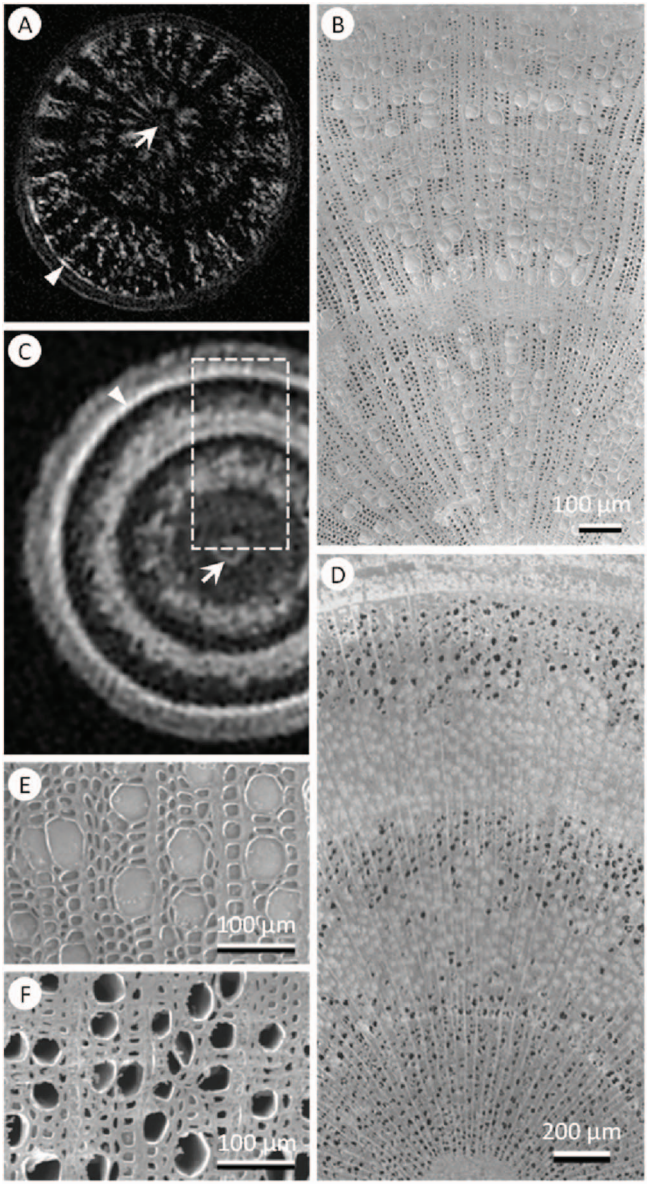

Figure 1. Typical cross-sectional images of MRI and cryo-SEM observations. (A) Magnetic resonance image of *C. tschonoskii* with Ψ_{leaf} of −2.0 MPa. The water-containing regions are white, whereas waterless regions are dark. Arrowhead, cambial zone; arrow, pith. (B) Cryo-SEM image of *C. tschonoskii* xylem without gas-filled vessels. (C) Magnetic resonance image of *C. japonicum* with Ψ_{leaf} of −2.2 MPa. (D) Cryo-SEM image of *C. japonicum* in the box field shown in (C). (E) Magnified view of a water-filled xylem of *C. japonicum* with Ψ_{leaf} of −1.3 MPa. (F) Magnified view of a xylem of *C. japonicum* with Ψ_{leaf} of −2.2 MPa.

cutting. Branch samples at the MR imaging point were frozen with LN_2 and stored at −80 °C until cryo-SEM observation (see above).

The luminance of each MR image was standardized using iPlus image display software (MRTechnology Inc.) to diminish background noise and standardize the brightness of the background among the images. Two MR images were stacked, automatically positioned using the StackReg plugin (Thévenaz et al. 1998) and then subtracted from each other using the image calculator tool in ImageJ (National Institute of Mental Health, Bethesda, MD, USA) to compare water distributions.

Experiment 2: cryo-fixation artifact observations by cryo-SEM

The extent of cryo-fixation artifact formation caused by freezing samples with and without tension relaxation were investigated by observing xylem water content using cryo-SEM. Potted *C. tschonoskii* (n = 12) and *C. japonicum* (n = 10) samples were dehydrated by terminating irrigation. Plants with various dehydration levels were then transported to the laboratory a few days before the experiment was conducted to eliminate the diurnal course of Ψ_{leaf}. Half of the samples with Ψ_{leaf} ranging from −0.3 MPa to −3.3 MPa were frozen for 5 min with LN_2 through a plastic collar attached around a stem. For xylem tension relaxation, the remaining samples within the same range of Ψ_{leaf} were rehydrated by cutting the stems under water, which was filled in a plastic collar attached at the distal portion of a stem at a position beyond MVL from a freezing position (see Figure S1B available as Supplementary Data at *Tree Physiology* Online). Furthermore, Ψ_{leaf} was monitored two to three times in leaves expanded from a branch diverging from a basal portion of the stem until >-0.5 MPa. Approximately 1 h and 30 min was required for complete xylem tension relaxation in highly dehydrated samples of *C. tschonoskii* (Ψ_{leaf} <-3 MPa) or *C. japonicum* (Ψ_{leaf} <-2 MPa), respectively. Stem freezing of each tension-relaxed sample was conducted as described above. The freezing position of the tension-relaxed samples was the same as that of samples without tension relaxation. Specimens excised from frozen stem samples were stored at −80 °C until their xylem water distribution was observed using cryo-SEM.

Another set of branches collected from field-grown plants was frozen at a rate of −4.3 °C h^{-1}, which is the natural rate in cold regions (Cordero and Nilsen 2002, Mayr et al. 2007), using a program chamber (MC-711, Espec Corp., Osaka, Japan) to clarify differences in xylem lumen contents between samples slowly frozen in a program chamber and rapidly frozen using LN_2. One of the two slowly frozen branch samples of each species was bench-dried until a significant xylem tension was achieved. After freezing, specimens were excised and stored as described above.

All measured vessels were divided into five categories of lumen content to clarify the effects of xylem tension and its relaxation on the occurrence and magnitude of cryo-fixation artifacts within vessel lumina: (i) water-filled, (ii) fully empty, (iii) flat or convex water drop, (iv) water layer on vessel lumen or (v) clustering water (ice) particles after cryo-SEM observation of cross-sections of rapidly or slowly frozen cryo-fixed specimens. Numbers of each categorized vessel were counted in radial sectors (n = 1–3 per a cross-section), ranging from the pith to the cambium in each species. Cross-sections of 1-year-old (including current-year and 1-year-old xylem) samples were observed in both species. However, only the current-year xylem was analyzed in *C. japonicum* samples because most 1-year-old xylems of this species were already embolized during growth even under sufficient irrigation (see Figure 4). Vessels with lumen contents that could not be distinguished because of structural collapse during cryoplaning or frost debris on the viewing surface were excluded from the frequency analysis (such vessels were <0.1% of total vessels). The total number of vessels in each sector was observed to be 113–485 and 235–467 for *C. tschonoskii* and *C. japonicum*, respectively.

Statistics

The association between the frequency of each vessel content category and Ψ_{leaf} in samples with/without tension relaxation was fitted using a generalized linear mixed model (GLMM). The binominal distribution was used as a probability distribution for simplicity, and the logit link function was used as a link function. Xylem tension relaxation and Ψ_{leaf} were considered to be explanatory variables. The sectors that we analyzed in a cryo-SEM image were considered to be a random effect in each sample. The GLMM analysis was conducted using the GLMM function provided by the lme4 package (Bates et al. 2015), and the model yielding the smallest value of Akaike's information criterion was considered to be the best model. Model fitting was performed using R software (Version 3.2.3, R Development Core Team).

Results

Maximum vessel length

The MVL of *C. tschonoskii* and *C. japonicum* were 0.12 ± 0.01 m (mean ± SE, n = 3) and 0.27 ± 0.02 m (mean ± SE, n = 4), respectively. For tension relaxation treatment, branches/stems were cut at a position farther from or near the MR imaging point, i.e., greater or lesser than MVL, respectively.

Vessel content in MR and cryo-SEM images

Water-filled vessels were visualized as white patches in the MR images compared with the cryo-SEM images of *C. tschonoskii* (Figure 1A and B). Regions without vessels consisting of radial/axial parenchyma and empty wood fibers in the xylem were visualized as black patches because these regions contain less water per pixel than water-filled vessels. Water-filled

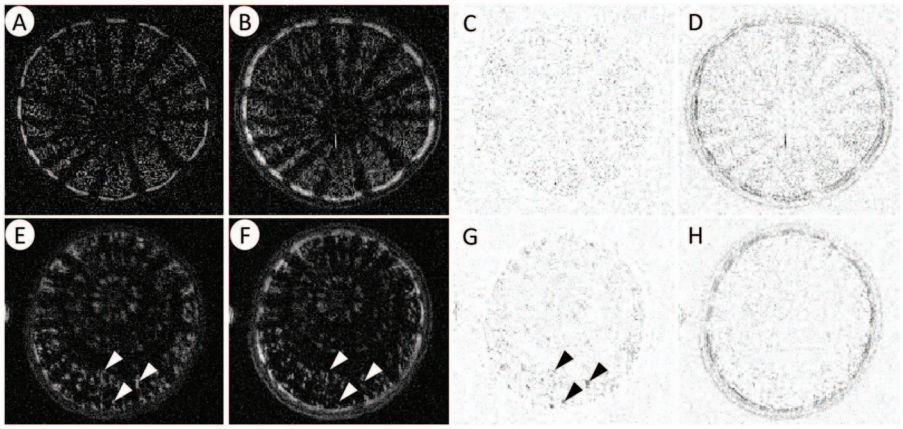

Figure 2. Magnetic resonance images of branch cross-sections and the subtracted images in *C. tschonoskii* samples with the axis cut at a position <MVL from the MR imaging point (A–D) and at a position >MVL from the MR imaging point (E–H). Magnetic resonance images acquired before (A) and after (B) tension relaxation, with Ψ_{leaf} recovered from −2.65 MPa to −0.25 MPa. Magnetic resonance images acquired before (E) and after (F) tension relaxation, with Ψ_{leaf} recovered from −2.85 MPa to −0.5 MPa. (C, G) Results of image subtraction of (A, E) from (B, F), respectively. (D, H) Results of image subtraction of (B, F) from (A, E), respectively. Arrowheads in panels (E–G) indicate examples of vessel cavitation.

xylem regions were visualized as bright areas in *C. japonicum* (Figure 1C and D). These regions comprised water-filled vessels and fiber tracheids (Figure 1E). On dehydration, the fiber tracheids in this species became empty after vessel cavitation (Figure 1F). In both species, the cambial zone and pith were visualized as a bright ring and bright zone, respectively (Figure 1A and C).

Xylem embolism and refilling after xylem tension relaxation

Xylem water distribution in a *C. tschonoskii* sample (Ψ_{leaf} = −2.65 MPa) showed no change within 1 h after releasing xylem tension (Ψ_{leaf} = −0.25 MPa) by cutting back the basal end of the branch under water at a position near (<MVL) the MR imaging point (Figure 2A–D; Figure S2 in two other samples, available as Supplementary Data at *Tree Physiology* Online). When a sample (Ψ_{leaf} = −2.85 MPa) was cut under water at a position farther (>MVL) from the MR imaging point, a small portion of water-filled vessels disappeared in two of three samples (Figure 2E–H, arrowheads; Figure S3 in two other samples, available as Supplementary Data at *Tree Physiology* Online), and Ψ_{leaf} recovered to −0.50 MPa.

Over 1 h following xylem tension relaxation, empty vessels, particularly those with small diameters surrounding the pith, were refilled with water in all three samples cut at a position near (<MVL) the MR imaging point (Figure 3A–D, arrowheads; Figure S2 available as Supplementary Data at *Tree Physiology* Online). One of the three samples cut at a position farther (>MLV) from the MR imaging point showed partial xylem refilling (Figure 3E and F; Figure S3 available as Supplementary Data at *Tree Physiology* Online), and the refilling region expanded with time (Figure 3F–H).

In *C. japonicum*, no tension-cutting artifact was observed within 30 min after a sample (Ψ_{leaf} = −1.95 MPa) was cut under water at a position near (<MVL) the MR imaging point (Ψ_{leaf} = −0.25 MPa, Figure 4A–C; Figure S4 in the two other samples, available as Supplementary Data at *Tree Physiology* Online). The same results were obtained when a sample (Ψ_{leaf} = −1.95 MPa) was cut at a position farther (>MVL) from the MR imaging point (Ψ_{leaf} = −0.40 MPa, Figure 4E–G; Figure S5 in two other samples, available as Supplementary Data at *Tree Physiology* Online). In contrast, in two of the three samples for each treatment, small increases in luminance at an embolized region in 1-year-older xylem were detected after rehydration (Figure 4A, B, E and F, arrowheads; Figures S4 and S5 available as Supplementary Data at *Tree Physiology* Online), shown as light gray patches in the subtracted images (Figure 4D and H). The corresponding region comprised both water- and gas-filled vessels and water-filled fiber tracheids (Figure 5) observed using cryo-SEM.

Effect of xylem tension relaxation on the occurrence and magnitude of cryo-fixation artifacts

When drought-stressed *C. tschonoskii* and *C. japonicum* samples were frozen using LN_2 with or without tension relaxation, various states in the vessel lumina were observed in the cryo-SEM images. Unlike the empty vessels (Figure 6, arrowhead #2), water-filled vessel lumina were observed as flat surfaces of water at the transverse plane (Figure 6, arrowhead #1). In addition, vessels with a (few) flat or convex water drop(s) inside the lumina were observed, particularly in stressed samples (Figure 6, arrowhead #3). In rare cases, a ring-like pool of water could be observed inside the lumen (Figure 6D, arrowhead #4). Interestingly, vessels with clustering water particles inside the lumina were frequently observed in samples frozen using LN_2 without xylem tension relaxation (Figure 6, arrowhead #5).

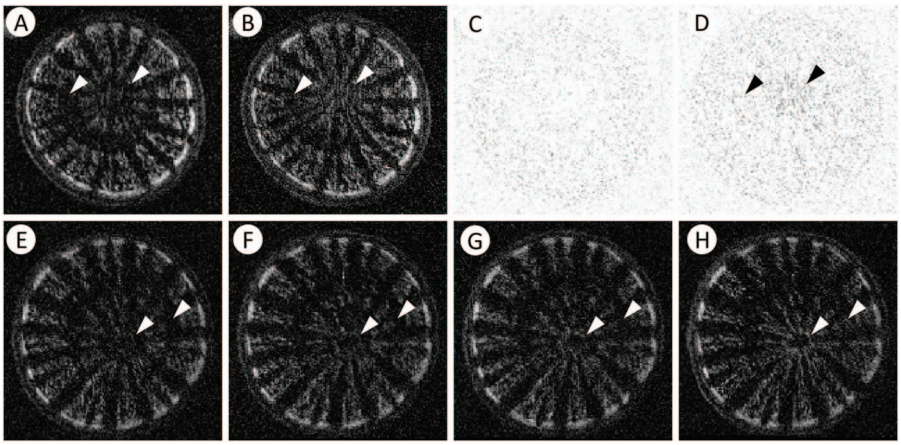

Figure 3. Magnetic resonance images of branch cross-sections and the subtracted images of *C. tschonoskii* samples obtained periodically after tension relaxation treatment. (A, B) Magnetic resonance images acquired at 1 h and 2 h after tension relaxation in a sample with the axis cut at a position <MVL from the MR imaging site, with Ψ_{leaf} recovered from −2.85 MPa to −0.15 MPa in 1 h. (C) Results of image subtraction of (A) from (B). (D) Results of image subtraction of (B) from (A). (E–H) Magnetic resonance images acquired at 1, 2, 3 and 12 h after tension relaxation of a sample with the axis cut at a position >MVL from the MR imaging site, with Ψ_{leaf} recovered from −2.15 MPa to −0.25 MPa in 1 h. Arrowheads in each panel indicate a refilled xylem region in each sample.

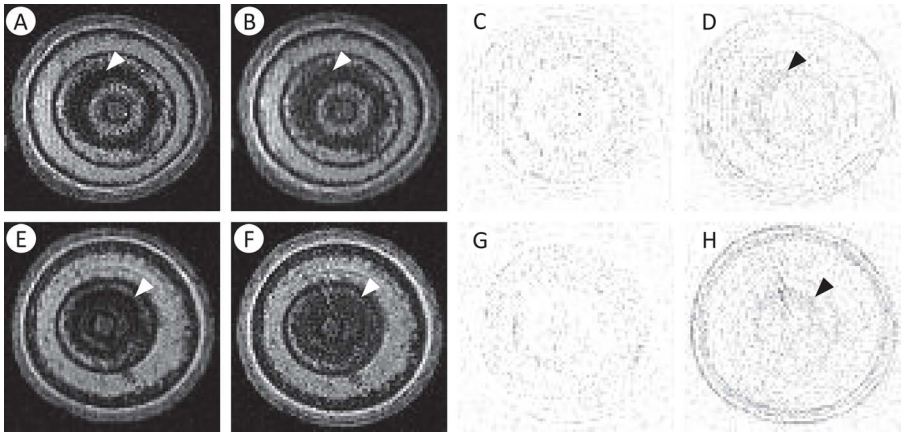

Figure 4. Magnetic resonance images of branch cross-sections and the subtracted images of *C. japonicum* samples with the axis cut at a position <MVL from the MR imaging site (A–D) and at a position >MLV from the MR imaging site (E–H). Magnetic resonance images acquired before (A) and after (B) tension relaxation, with Ψ_{leaf} recovered from −1.95 MPa to −0.25 MPa. Magnetic resonance images acquired before (E) and after (F) tension relaxation, with Ψ_{leaf} recovered from −1.95 MPa to −0.4 MPa. (C, G) Results of image subtraction of (A, E) from (B, F). (D, H) Results of subtraction of (B, F) from (A, E). Arrowheads indicate an example of a refilled region in the xylem.

In *C. tschonoskii* samples, the relative number of water-filled vessels in samples frozen using LN_2 without tension relaxation decreased from 80% as Ψ_{leaf} decreased below −2 MPa; however, those of samples frozen after tension relaxation remained >90% at similar Ψ_{leaf} (Figure 7A). The relative number of fully empty vessels or vessels containing water drops with flat or convex shapes increased with decreasing Ψ_{leaf} in samples frozen using LN_2 without xylem tension relaxation (Figure 7B and C). Interestingly, despite a decrease in Ψ_{leaf}, the numbers of such vessels were <10% in samples frozen using LN_2 with xylem tension relaxation. Vessels surrounded by water inside the lumen were relatively rare (<1%) and independent of Ψ_{leaf} in samples frozen using LN_2 with or without xylem tension relaxation; however, the numbers were slightly higher in samples frozen without xylem tension relaxation (Figure 7D). Vessels with clustering water particles appeared randomly in samples frozen using LN_2 without xylem tension relaxation; however, they were limited (i.e., near-zero levels) in samples with xylem tension relaxation (Figure 7E). Although 20% of vessels were embolized even under moist conditions (Ψ_{leaf} >−0.5 MPa) in *C. japonicum* samples frozen after xylem tension relaxation (Figure 7F), associations between Ψ_{leaf} and the relative number of each type of vessels were similar to those in *C. tschonoskii* samples (Figure 7G–J).

In *C. tschonoskii*, fewer water-filled vessels were observed in samples slowly frozen at a rate of −4.3 °C h^{-1}, than in samples frozen using LN_2 with xylem tension relaxation (Figure 7A). Vessel lumina with water drops or clustering water particles were

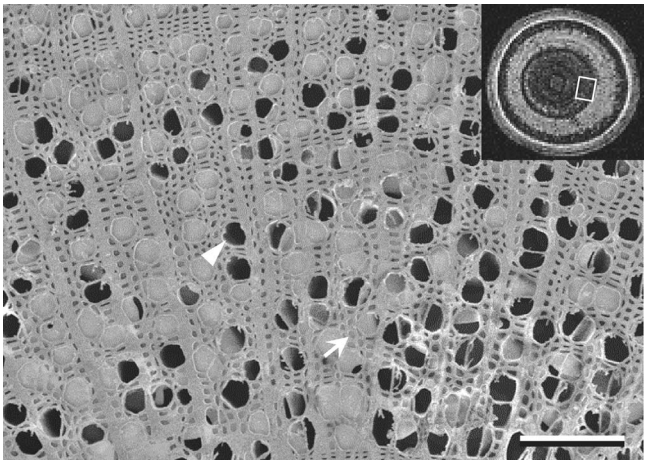

Figure 5. Cryo-SEM image corresponding to an MR image of the *C. japonicum* sample shown in Figure 4E–H. The xylem water content of this sample increased based on differential analysis of MR images acquired before and after tension relaxation. The bottom of the cryo-SEM image is the pith side. Arrowhead, empty vessels; arrow, water-filled fiber tracheids. Scale bar, 100 μm.

rarely observed (<8%) in slowly frozen samples (Figure 7C and E); however, vessel lumina with a ring-like pool of water were more frequently observed in slowly frozen samples than in those frozen using LN_2 (Figure 7D). Moreover, similar results were found in slowly frozen *C. japonicum* samples (Figure 7F–J).

Discussion

The effect of cutting on xylem water distribution was observed to be negligible in the studied species, although the samples were under tension. In *C. tschonoskii*, the water loss in the vessel lumen was observed in two of three branch samples cut at a position farther (>MVL) from the MR imaging point. In contrast, water loss in the vessel lumen was not observed in all of the three samples cut at a point <MVL from the MR imaging point, although this treatment is expected to induce severe tension-cutting artifacts (Figure 2; Figure S2 available as Supplementary Data at *Tree Physiology* Online). These results suggest that the water loss in the vessel lumen observed in the two *C. tschonoskii* samples is caused not by tension-cutting artifacts but by drought-induced cavitation during MR image capture. Moreover, Ψ_{leaf} of samples with partial xylem water loss was −2.9 MPa, which is a value that causes runaway embolism in this species (Ogasa et al. 2013). In *C. japonicum*, no water loss in the vessel lumen was observed after samples were cut under water at negative pressure regardless of the cutting point (Figure 4).

Our results revealed that vessel refilling rarely occurs during short-term rehydration and that long-term rehydration should be avoided because vessel refilling occurs. In *C. tschonoskii*, refilling occurred in vessels with small diameters surrounding the pith

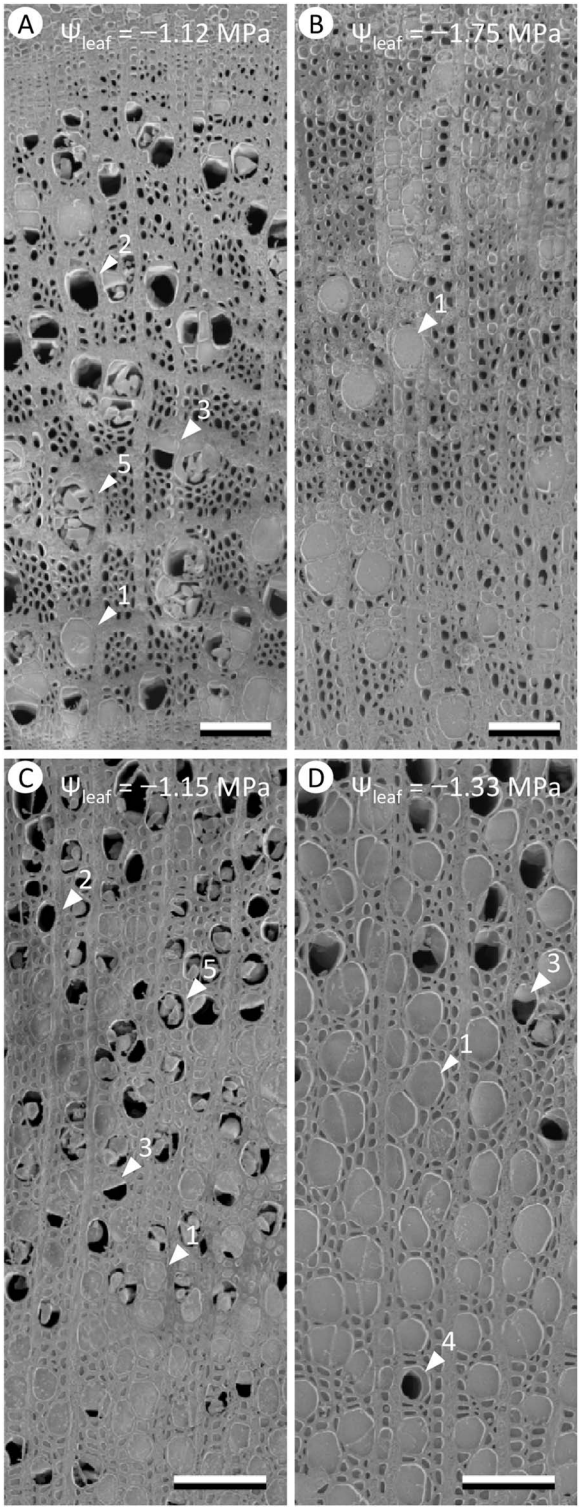

Figure 6. Cryo-SEM images of samples without tension relaxation (A, C) and with tension relaxed before freezing with LN_2 (B, D) in *C. tschonoskii* (A, B) and *C. japonicum* (C, D). The Ψ_{leaf} of each sample is shown in each panel. Numbers in each panel represent: #1, water-filled vessel; #2, fully empty vessel; #3, vessel containing flat or convex water drop(s); #4, vessel with ring-like water inside the lumen; and #5, vessel with clustering water particles. Scale bar, 100 μm.

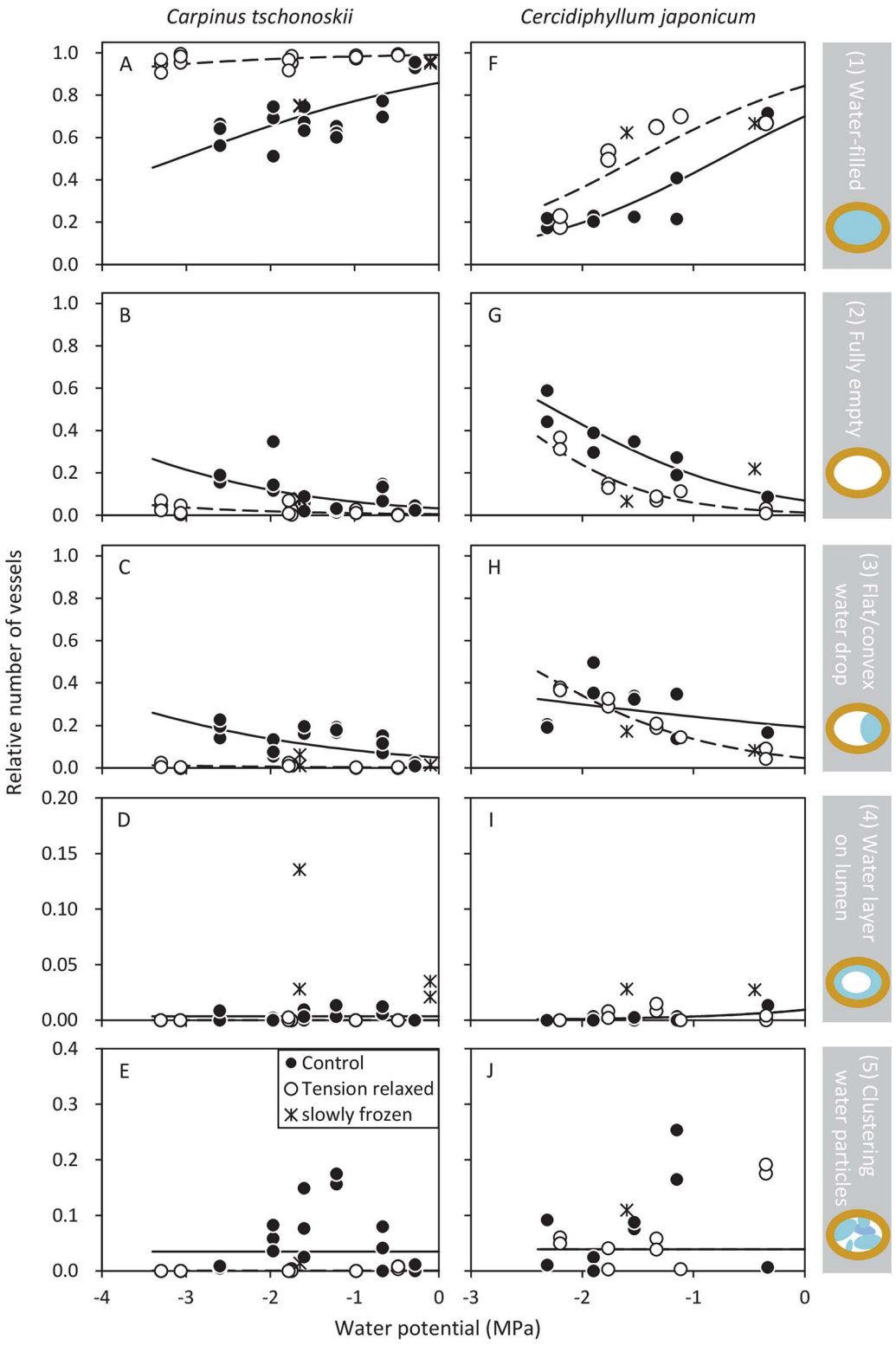

Figure 7. Associations between leaf water potential and frequency of each vessel lumen category in stem xylems frozen using LN_2 (control, closed symbols and solid line) or LN_2 after xylem tension release (tension-relaxed, open symbols and dashed line) in potted saplings of *C. tschonoskii* (A–E) and *C. japonicum* (F–J). The categories of vessel lumen and the corresponding pattern diagram are indicated in the gray column on the right. Asterisk symbols in each panel represent similar data from the large cut branch slowly frozen in a program chamber and excluded from curve fitting. In samples with tension relaxation before LN_2 freezing, the values of leaf water potential exactly before tension relaxation are plotted in each graph.

and in vessels with small diameter in the three samples that were cut at a position near the MRI point and in one of three samples cut at a position >MVL from the MR imaging point. Differences in the probability of refilling between the two cutting treatments imply that vessel refilling during long-term rehydration is caused by capillary rise and not by physiological processes associated with xylem living-cell activity, as reported previously (Brodersen et al. 2010, Secchi and Zwieniecki 2011). Although the time period required to refill air-filled vessels or fiber tracheids is species-specific, long-term rehydration for xylem tension relaxation and tension-cutting artifact prevention must be performed with caution to maintain the in vivo xylem water distribution (Canny et al. 2001, Trifilò et al. 2014, Ogasa et al. 2016).

In *C. japonicum*, a slight increase in luminance was detected after cutting under water in two of the three samples for both cutting treatments (Figure 4; Figures S4 and S5 available as Supplementary Data at *Tree Physiology* Online). Compared with the xylem water distribution in *C. tschonoskii*, in which lumen water was observed in vessels only, lumen water was present in both vessels and fiber tracheids in *C. japonicum* (Figure 1). Considering that the luminance of a pixel is determined by water content per voxel (67 μm × 67 μm × 1 mm) that contains both vessels and fiber tracheids dimensionally in *C. japonicum* (Figure 1E and F), increased luminance may be induced by an increase in water content per voxel following partial vessel or fiber tracheid refilling in gas-filled regions in the xylem.

We confirmed that cryo-fixation artifacts are produced extensively if xylem tension relaxation is not performed before LN_2-plunge freezing, as previously reported in leaf petioles (Cochard et al. 2000) and seedling stems (Umebayashi et al. 2015). Based on the results of Experiment 1 (MRI experiment), rehydration exerts minor effects of cutting/refilling artifacts on the xylem water distribution in *C. tschonoskii* (1 h rehydration) and *C. japonicum* (30 min rehydration). Therefore, we can assume that the results of experiment 2 (cryo-SEM observations) are barely involved in these effects. Differences in the number of water-filled vessels between the tension relaxation-treated samples and controls resulted from the impact of the freezing procedure itself, that is, vessel cavitation was caused by freezing samples that remained under tension.

Increased empty vessels or vessels with water drops were associated with increased xylem tension in control samples of both species because of the interaction between xylem tension and air bubbles expelled from xylem water during freezing. Plant hydraulic systems are usually under tension and, thus, in a metastable state (Dixon and Joly 1895, Tyree and Zimmermann 2002). During freezing under such a status, ice nuclei can be produced and can grow larger. Moreover, micro air bubbles expelled from unfrozen water can expand. Thus, water-filled vessels hold air space in their lumen after samples are frozen (Lybeck 1959, Cochard et al. 2000). The former process is independent of the intensity of negative pressure. The air volume expelled from unfrozen xylem water is independent of the intensity of negative pressure because the solubility of air is much lower in ice than in water (1000×; Scholander et al. 1953). The latter process is associated with the extent of negative pressure. In particular, air bubbles are pulled down by unfrozen tensioned water, resulting in their expansion; this can be the main cause of cryo-fixation artifacts with increasing negative pressure (Cochard et al. 2000, Umebayashi et al. 2015).

Vessel contents, termed cryo-fixation artifacts in the present study (Figure 6, arrowheads #2 and #3), except for vessels containing clustered water particles, have been identified in situ in some woody species (e.g., *Betula platyphylla* var. *japonica*, *Fraxinus mandshurica* var. *japonica* and *Vitis vinifera* in Utsumi et al. 1998, 1999, Brodersen et al. 2010). Previous findings suggest that complete identification of whether the vessel content status is induced by cryo-fixation artifacts or occurs naturally under native conditions is challenging. Vessel lumina with a water layer were specifically found in samples slowly frozen in the program chamber and not in samples frozen using LN_2. This could be because slow freezing rates produce air bubbles with larger diameters, and expelled air bubbles can grow into air columns as the xylem water freezes (Bari and Hallett 1974, Utsumi et al. 1999, Sevanto et al. 2012).

Cryo-fixation artifacts cannot be completely eliminated even if xylem tension relaxation is performed before freezing, although the effect of artifacts on the xylem water distribution may only be minor. In Experiment 2 (cryo-SEM observations), samples to be rehydrated were cut under water at a downstream position from the cryo-SEM observation site (see Figure S1B available as Supplementary Data at *Tree Physiology* Online). The open vessels at the cut end with xylem tension relaxation were fewer in this case than in samples that were cut and rehydrated at an upstream position from the intended site. The extent of tension relaxation in intact vessels can depend on the hydraulic connection of these vessels with open vessels at the cut end. Species-specific hydraulic pathways through vessel networks may explain differences in the relieving effect of cryo-fixation artifacts by tension relaxation between species.

Our data reveal that short-time xylem tension relaxation attenuates the effects of tension-cutting, refilling and cryo-fixation artifacts on xylem water distribution in species with short vessels. In species with long vessels, both major and minor effects of tension-cutting artifacts have been reported (Wheeler et al. 2013, Venturas et al. 2014, Torres-Ruiz et al. 2015, Ogasa et al. 2016). Although no study has investigated the effects of cryo-fixation artifacts in species with long vessels, these effects may be severe considering the amount of gas dissolved in a long vessel compared with that in a short vessel. When investigating xylem transport function or xylem water distribution in plant species, preliminary experiments are required to obtain an awareness regarding species-specific sampling artifacts.

Supplementary Data

Supplementary Data for this article are available at *Tree Physiology* Online.

Acknowledgments

We thank Dr Tomoyuki Haishi (MRTechnology Inc., Tsukuba) for technical support with MR image analysis and Dr Kabeya Daisuke (Forestry and Forest Products Research Institute, Tsukuba) for technical advice of statistics. We also thank two anonymous reviewers for their helpful comments.

Conflict of interest

None declared.

Funding

This work was supported by JSPS KAKENHI Grant Numbers JP23248022, JP15H02450, JP25850102 and JP14J08279, and by Research Grant Number 201706 of the Forestry and Forest Products Research Institute.

References

Bari SA, Hallett J (1974) Nucleation and growth of bubbles at an ice-water interface. J Glaciol 13:489–520.

Bates D, Maechler M, Bolker B, Walker S (2015) Fitting linear mixed-effects models using lme4. J Stat Softw 67:1–48.

Brodersen CR, McElrone AJ, Choat B, Matthews MA, Shackel KA (2010) The dynamics of embolism repair in xylem: in vivo visualizations using high-resolution computed tomography. Plant Physiol 154:1088–1095.

Canny MJ, McCully ME, Huang CX (2001) Cryo-scanning electron microscopy observations of vessel content during transpiration in walnut petioles. Facts or artefacts? Plant Physiol Biochem 39:555–563.

Cobb AR, Choat B, Holbrook NM (2007) Dynamics of freeze-thaw embolism in *Smilax rotundifolia* (Smilacaceae). Am J Bot 94:640–649.

Cochard H, Tyree MT (1990) Xylem dysfunction in *Quercus*: vessel sizes, tyloses, cavitation and seasonal changes in embolism. Tree Physiol 6:393–407.

Cochard H, Bodet C, Améglio T, Cruiziat P (2000) Cryo-scanning electron microscopy observations of vessel content during transpiration in walnut petioles. Plant Physiol 124:1191–1202.

Cochard H, Delzon S, Badel E (2014) X-ray microtomography (micro-CT): a reference technology for high-resolution quantification of xylem embolism in trees. Plant Cell Environ 38:201–206.

Cordero RA, Nilsen ET (2002) Effects of summer drought and winter freezing on stem hydraulic conductivity of *Rhododendron* species from contrasting climates. Tree Physiol 22:919–928.

Dixon HH, Joly J (1895) On the ascent of sap. Philos Trans R Soc London B 186:563–576.

Fukuda K, Kawaguchi D, Aihara T, Ogasa MY, Miki NH, Haishi T, Umebayashi T (2015) Vulnerability to cavitation differs between current-year and older xylem: non-destructive observation with a compact magnetic resonance imaging system of two deciduous diffuse-porous species. Plant Cell Environ 38:2508–2518.

Lybeck BR (1959) Winter freezing in relation to the rise of sap in tall trees. Plant Physiol 34:482–486.

Mayr S, Cochard H (2003) A new method for vulnerability analysis of small xylem areas reveals that compression wood of Norway spruce has lower hydraulic safety than opposite wood. Plant Cell Environ 26:1365–1371.

Mayr S, Cochard H, Améglio T, Kikuta SB (2007) Embolism formation during freezing in the wood of *Picea abies*. Plant Physiol 143:60–67.

Melcher P (2015) Seeing into the xylem using non-invasive techniques provides clarity in understanding mechanisms involved in long-distance sap transport in plants. Plant Cell Environ 38:2497–2499.

Nagai S, Utsumi Y (2012) The function of intercellular spaces along the ray parenchyma in sapwood, intermediate wood, and heartwood of *Cryptomeria japonica* (Cupressaceae). Am J Bot 99: 1553–1561.

Ogasa M, Miki NH, Murakami Y, Yoshikawa K (2013) Recovery performance in xylem hydraulic conductivity is correlated with cavitation resistance for temperate deciduous tree species. Tree Physiol 33:335–344.

Ogasa MY, Utsumi Y, Miki NH, Yazaki K, Fukuda K (2016) Cutting stems before relaxing xylem tension induces artefacts in *Vitis coignetiae*, as evidenced by magnetic resonance imaging. Plant Cell Environ 39:329–337.

Rockwell FE, Wheeler JK, Holbrook NM (2014) Cavitation and its discontents: opportunities for resolving current controversies. Plant Physiol 164:1649–1660.

Sano Y, Okamura Y, Utsumi Y (2005) Visualizing water-conduction pathway of living trees: selection of dyes and tissue preparation methods. Tree Physiol 25:269–275.

Savi T, Miotto A, Petruzzellis F, Losso A, Pacile S, Tromba G, Mayr S, Nardini A (2017) Drought-induced embolism in stems of sunflower: a comparison of in vivo micro-CT observations and destructive hydraulic measurements. Plant Physiol Biochem 120:24–29.

Scholander PF, Flagg W, Hock RJ, Irving L (1953) Studies on the physiology of frozen plants and animals in the arctic. J Cell Comp Physiol 42:(Supp 1)1–56.

Scholander PF, Hammel HT, Bradstreet ED, Hemmingsen EA (1965) Sap pressure in vascular plants. Science 148:339–346.

Scoffoni C, Sack L (2015) Are leaves 'freewheelin'? Testing for a wheeler-type effect in leaf xylem hydraulic decline. Plant Cell Environ 38:534–543.

Secchi F, Zwieniecki MA (2011) Sensing embolism in xylem vessels: the role of sucrose as a trigger for refilling. Plant Cell Environ 34:514–524.

Sevanto S, Holbrook NM, Ball MC (2012) Freeze/thaw-induced embolism: probability of critical bubble formation depends on speed of ice formation. Front Plant Sci 3:107.

Sperry JS, Donnelly JR, Tyree MT (1988) A method for measuring hydraulic conductivity and embolism in xylem. Plant Cell Environ 11:35–40.

Thévenaz P, Ruttimann UE, Unser M (1998) A pyramid approach to subpixel registration based on intensity. IEEE Trans Image Process 7: 27–41.

Torres-Ruiz JM, Jansen S, Choat B et al. (2015) Direct x-ray microtomography observation confirms the induction of embolism upon xylem cutting under tension. Plant Physiol 167:40–43.

Trifilò P, Raimondo F, Lo Gullo MA, Barbera PM, Salleo S, Nardini A (2014) Relax and refill: xylem rehydration prior to hydraulic measurements favours embolism repair in stems and generates artificially low PLC values. Plant Cell Environ 37:2491–2499.

Turner NC (1988) Measurement of plant water status by the pressure chamber technique. Irrig Sci 9:289–308.

Tyree MT, Sperry JS (1989) Vulnerability of xylem to cavitation and embolism. Annu Rev Plant Physiol 40:19–38.

Tyree MT, Zimmermann MH (2002) Xylem structure and the ascent of sap, 2nd edn. Springer, Berlin, Germany.

Umebayashi T, Ogasa MY, Miki NH, Utsumi Y, Haishi T, Fukuda K (2015) Freezing xylem conduits with liquid nitrogen creates artifactual embolisms in water-stressed broadleaf trees. Trees 30:305–316.

Utsumi Y, Sano Y (2014) Freeze stabilization and cryopreparation technique for visualizing the water distribution in woody tissues by X-ray imaging and cryo-scanning electron microscopy. Methods Mol Biol 1117:677–688.

Utsumi Y, Sano Y, Fujikawa S, Funada R, Ohtani J (1998) Visualization of cavitated vessels in winter and refilled vessels in spring in diffuse-porous trees by cryo-scanning electron microscopy. Plant Physiol 117: 1463–1471.

Utsumi Y, Sano Y, Funada R, Ohtani J, Fujikawa S (1999) The progression of cavitation in earlywood vessels of *Fraxinus mandshurica* var *japonica* during freezing and thawing. Plant Physiol 121:897–904.

Utsumi Y, Sano Y, Funada R, Ohtani J, Fujikawa S (2003) Seasonal and perennial changes in the distribution of water in the sapwood of conifers in a sub-frigid zone. Plant Physiol 131:1826–1833.

Venturas MD, Mackinnon ED, Jacobsen AL, Pratt RB (2014) Excising stem samples underwater at native tension does not induce xylem cavitation. Plant Cell Environ 38:1060–1068.

Venturas MD, Sperry JS, Hacke UG (2017) Plant xylem hydraulics: what we understand, current research, and future challenges. J Integr Plant Biol 59:356–389.

Wheeler JK, Huggett BA, Tofte AN, Rockwell FE, Holbrook NM (2013) Cutting xylem under tension or supersaturated with gas can generate PLC and the appearance of rapid recovery from embolism. Plant Cell Environ 36:1938–1949.

Yazaki K, Ogasa MY, Kuroda K, Utsumi Y, Kitin P, Sano Y (2019) Xylem water distribution in woody plants visualized with a cryo-scanning electron microscope. JoVE :e59154.

Yazaki K, Takanashi T, Kanzaki N, Komatsu M, Levia DF, Kabeya D, Tobita H, Kitao M, Ishida A (2017) Pine wilt disease causes cavitation around the resin canals and irrecoverable xylem conduit dysfunction. J Exp Bot 69:589–602.

Zimmerman MH, Jeje AA (1981) Vessel-length distribution in stems of some American woody plants. Can J Bot 59:1882–1892.